Modulation of E-Cadherin Monomer Folding by Cooperative Binding of Calcium Ions†

Olivier Courjean,‡,⊥ Guillaume Chevreux,§ Emilie Perret,‡ Anne Morel,‡ Sarah Sanglier,§ Noelle Potier,§ Jürgen Engel,|| Alain van Dorsselaer,§ and Hélène Feracci*,‡,⊥

Centre de Recherche Paul Pascal, Université Bordeaux 1, CNRS UPR 8641, 115 Avenue du Dr. Schweitzer, Pessac, France and Morphogenèse cellulaire et progression tumorale, Institut Curie, CNRS UMR 144, Paris, France, Laboratoire de Spectrométrie de Masse Bio-Organique, Institut Pluridisciplinaire Hubert Curien, UMR 7178 CNRS-Université Louis Pasteur, Strasbourg Cedex 2, France, and Department of Biophysical Chemistry, Biozentrum Universitaet Basel, Basel, Switzerland

Received July 7, 2007; Revised Manuscript Received October 10, 2007

ABSTRACT: Classical cadherins are transmembrane glycoproteins involved in calcium-dependent cell−cell adhesion. Calcium ions are coordinated at the interface between successive modules of the cadherin ectodomain and are thought to regulate the adhesive interactions of cadherins when present at millimolar concentrations. It is widely accepted that calcium plays a critical role in cadherin-mediated cell−cell adhesion, but the nature of cadherin−calcium binding remains a matter of debate. We investigated the parameters of noncovalent cadherin−calcium binding, using the two N-terminal modules of E-cadherin (E/EC12) with a native N-terminal end and nondenaturing electrospray ionization mass spectrometry. By directly visualizing the molecular complexes, we demonstrated that E/EC12 binds three calcium ions, with an average K_D of 20 ± 0.7 μM. These calcium ions bound cooperatively to E/EC12 in its monomeric state, and these properties were not modified by an N-terminal extension consisting of a single methionine residue. This binding induced specific structural changes, as shown by assessments of protease sensitivity, circular dichroism, and mass spectrometry. Furthermore, the D103A mutation (a residue involved in E-cadherin adhesive function) modified calcium binding and led to a loss of cooperativity and the absence of structural changes, despite calcium binding. As the amino acids involved in calcium binding are found within the cadherin consensus motif, our findings may be relevant to other members of the cadherin family.

Cell−cell interactions play crucial roles in cell differentiation, tissue morphogenesis, and signal transduction (*1*−*3*). These interactions appear to be mediated by specific contacts between adhesion receptors on the apposing cell membranes (*4*). These receptors include molecules of different classes, responsible for various mechanisms of cellular adhesion. Cadherins are unique among these receptors, in that they are responsible for Ca^{2+}-dependent homophilic adhesion between cells (*5*−*7*). Classical cadherins include ∼20 single-pass transmembrane glycoproteins with an extracellular segment consisting of five similar tandemly arranged cadherin domains (EC),[1] named EC1−EC5, starting from the N-terminal end (*8*). These domains have similar sequences and an Ig-like structure consisting of seven antiparallel β-strands organized into two opposing sheets (*9*−*11*). The adhesive activity of cadherins at the cellular level is regulated by several mechanisms, including activation by cleavage, protein expression at the plasma membrane, recruitment to cell contact zones, internalization, cadherin−calcium binding, and interactions with the cytoskeletal network (*12*−*16*).

The questions underlying most studies of cadherin-mediated adhesion at the molecular level concern the determinants of cadherin specificity and the role of calcium in cadherin-mediated interactions (*15*, *17*−*19*). Studies of calcium-dependent cell adhesion led to the discovery and characterization of the first cadherin, E-cadherin (for epithelial cadherin), previously known as uvomorulin. Early studies demonstrated that E-cadherin played an essential role in the compaction of embryonic cells with calcium ions (*20*). Cell aggregation studies have confirmed that calcium is essential for E-cadherin-mediated adhesion, which is reversibly inactivated by EDTA (*21*). All classical cadherins have a number of features in common: a very similar domain organization and a number of key residues, some of which are involved in Ca^{2+} binding (*8*). Mutations in these Ca^{2+}-binding sites modify the adhesive properties of E-cadherin.

† This work was supported by CNRS institutional funding and through the Protéomique et Génie des Protéines program, Institut Curie, and grants from Région Aquitaine, l'Association pour la Recherche contre le Cancer, Gefluc, la Fondation pour la Recherche Médicale, and la Ligue Contre le Cancer-Dordogne (grant to H.F.). O.C. held a BDI fellowship from the CNRS, the ARC, and from la Ligue Contre le Cancer-Oise. G.C. thanks the CNRS and Sanofi-Aventis for financial support.

* To whom correspondence should be addressed. Telephone: (33) 5 56 84 30 26. Fax: (33) 5 56 84 56 00. E-mail: feracci@crpp-bordeaux.cnrs.fr.

‡ CNRS UMR 144.

⊥ CNRS UPR 8641.

§ UMR 7178 CNRS-Université Louis Pasteur.

|| Biozentrum Universitaet Basel.

[1] Abbreviations: EC, cadherin extracellular module; EC12, two outermost extracellular domains of cadherins; EC15, five extracellular domains of cadherins; E/EC12 and E/EC15, E-cadherin EC12 and EC15 fragments, respectively; MR-E/EC12 or M-E/EC12, E-cadherin EC12 fragments containing additional Met-Arg or Met amino acids, respectively, at the N-terminal end with respect to the native sequence.

10.1021/bi701340d CCC: $40.75
Published on Web 01/31/2008

For example, mutations replacing Asp134 in the DXD motif of EC2, in the outermost binding pocket, with Ala or Lys abolish murine E-cadherin adhesion (*22*). Similarly, mutations converting the DXXD motif to DXXA in EC1 (Asp103 to Ala) or EC2 also markedly decrease the extent of homophilic adhesion (*23*, *24*).

Cadherin-mediated cell adhesion is thought to depend on the presence of calcium ions at millimolar concentrations, as in the extracellular medium (*25*). High-resolution structures of the extracellular fragments of E-, N-, and C-cadherin have shown that all the various binding pockets are organized similarly. Each pocket binds three Ca^{2+} ions, resulting in the binding to the complete structure of 12 calcium ions in total (see refs *10* and *19* for reviews). Calcium is required for cadherin structure, and in the presence of 50 μM Ca^{2+}, the extracellular E-cadherin segment (E/EC15) adopts a 22 nm protease-resistant rodlike shape (*26*, *27*). Cadherin modules display a secondary structure consisting largely of β-barrels in the presence of calcium, as shown by circular dichroism spectroscopy. Differences in the spectra obtained in the presence and absence of EDTA suggest that calcium may alter the secondary structure of the molecule (*28*).

The affinity of calcium for the extracellular E-cadherin domain has been evaluated with various fragments. The mean K_D of the four Ca^{2+}-binding pockets of E/EC15 has been reported to be 30−150 μM (*27*, *28*), depending on the method used. For the outermost Ca^{2+}-binding pocket, the three Ca^{2+} ions have a mean K_D of 20 ± 3 μM for binding to MR-E/EC12 (*29*) and a value of 55 ± 3 μM for binding to M-E/EC12 (*30*), contrasting with the mean K_D of 460 μM obtained for the same M-E/EC12 fragment (*28*). These findings suggest that a low-affinity Ca^{2+}-binding site (K_D of 2 mM) may be responsible for the physiological regulation of adhesive function by external calcium. These contradictory data concerning cadherin−calcium binding affinity led us to investigate the precise mechanisms underlying this calcium-induced regulation.

We focused on the outermost binding pocket, which is thought to contain a low-affinity binding site playing a major role in regulating the adhesive activity of E-cadherin. We used nondenaturing electrospray ionization mass spectrometry (ESI-MS), a powerful approach to studying protein−metal noncovalent interactions in solution (*31*−*34*), to investigate interactions between Ca^{2+} and cadherin fragments and to follow the structural rearrangements resulting from the binding of calcium ions. Under carefully controlled conditions, many studies have convincingly demonstrated that noncovalent complexes can survive the ionization−desorption process, providing important information about the stability and stoichiometry of the associations occurring in solution (*35*−*37*). ESI-MS can detect all species coexisting in solution and has therefore often been used to follow the pattern of protein−protein association and dissociation following the addition of ligand, or to investigate cooperativity effects (*32*, *38*−*41*). We found that three calcium ions bound, with a mean K_D of 20 ± 0.7 μM, to the EC12 interdomain pocket. This binding involved strong cooperativity with the E/EC12 cadherin fragment in its monomeric state (Hill coefficient of 2.6 ± 0.2) and induced specific changes in structure. The consequences of having an additional N-terminal methionine and/or a point mutation in this Ca^{2+}-binding pocket (D103A) were also investigated. We found that these additional residues had no significant effect on Ca^{2+} binding, despite potentially modifying cadherin interaction (*13*). By contrast, the Asp103 residue plays an essential role in this binding. Our data complement structural and biochemical studies (*28*−*30*, *42*) and provide new insight into the calcium-dependent adhesion mediated by cadherins.

EXPERIMENTAL PROCEDURES

Plasmid Constructions. The plasmid construct encoding the first two extracellular domains (M-E/EC12) fused to a C-terminal hexahistidine tag has been described previously (*43*). The sequence encoding this fragment was inserted between the *Xho*I and *Nde*I sites of pET24a. A point mutation was introduced into the M-E/EC12 sequence by QuickChange site-directed mutagenesis (Stratagene) with the following primers, D103A 5′-GTG ACA GAT CAG AAT GCC AAC AGG CCA-3′ and 5′-TGG CCT GTT GGC ATT CTG ATC TGT CAC-3′, to generate the M-E/D103A fragment. The constructs encoding the cleavable proteins MIEGR-E/EC12 (MXa-ECAD12) and MIEGR-E/D103A (MXa-E/D103A) were generated in two steps. Intermediate constructs were first obtained by inserting the HisXa sequence from pET19b(HisXa-ECAD12) (kindly provided by T. Ahrens and J. Engel; *14*) into pET24a(M-E/EC12) and pET24a(M-E/D103A), using the *Bgl*II and *Eco*RI sites and resulting in sequences encoding HisXa-E/EC12 and HisXa-E/D103A, respectively. HisXa contains a polyhistidine sequence and the four amino acids (IEGR) constituting the cleavage site of the factor Xa protease. Finally, the N-terminal polyhistidine tag was removed by excising the MIEGR-E/EC12 and MIEGR-E/D103A sequences from the intermediate plasmids and inserting them into pET24a, using the *Xho*I and *Nde*I sites. The cDNA constructs were sequenced to ensure that no undesirable mutations had arisen during cloning.

Protein Production and Purification. For production of the M-E/EC12, M-E/D103A, MIEGR-E/EC12, and MIEGR-E/D103 chimeric proteins, 500 mL of Terrific Broth supplemented with 50 μg/mL kanamycin was inoculated with a transformed colony picked from an agar plate. Proteins were produced as previously described (*43*). Cell pellets were resuspended in lysis buffer [4 M urea, 50 mM Na_2HPO_4 (pH 7.8), 20 mM imidazole, and 20 mM β-mercaptoethanol]. The resulting lysates were cleared by centrifugation, and the supernatant was incubated for 2 h with Ni-NTA Superflow agarose resin beads (Qiagen). The beads were thoroughly washed and subjected to stepwise dialysis against PBS.

Factor Xa protease digestion of 1 mg of MIEGR-E/EC12 or MIEGR-E/D103A chimeric protein [in 1 mL of a solution composed of 20 mM Tris, 50 mM NaCl, and 1 mM $CaCl_2$ (pH 6.5) supplemented with 50 units of factor Xa protease (Qiagen), for 60 h at 16 °C] was stopped by removing the enzyme with Xa Removal Resin (Qiagen). Fragments were then dialyzed against 20 mM Tris and 150 mM NaCl (pH 8) to remove Ca^{2+} ions and cleaved peptide. The cleaved proteins are termed E/EC12 and E/D103A, respectively.

Protein concentrations were determined spectrophotometrically, by determining absorbance at 280 nm. The molecular mass and absorbance coefficient of each protein were evaluated on the basis of amino acid composition, using the ProtParam tool from the ExPaSy web site (http://expasy.ch).

Protein Characterization. The isolated cadherin fragments were analyzed by SDS−PAGE in 15% polyacrylamide gels, followed by Coomassie blue staining. All proteins were characterized by Western immunoblotting. Two different primary antibodies were used: one directed against the EC1 module of E-cadherin (ECCD2, Takara) and the other directed against the C-terminal hexahistidine tag (His Probe H-15, Santa Cruz Biotechnology). Horseradish peroxidase (HRP)-linked whole antibodies were used as secondary antibodies (Amersham Biosciences), with photochemical detection via the ECL system (Amersham Biosciences).

Ca^{2+} Titration Monitored by Mass Spectrometry. Mass analyses were performed with an ESI-TOF mass spectrometer (LCT, Waters, Manchester, U.K.) calibrated with horse heart myoglobin (Sigma Aldrich, St. Louis, MO). Samples were continuously infused into the ESI ion source at a flow rate of 3 μL/min. Both the gas and source temperature were set at 353 K. Spectra were deconvoluted using the "transform" function of MassLynx.

For analysis under denaturing conditions, samples were diluted to a concentration of 2 pmol/μL in a 1:1 water/acetonitrile mixture (v/v) acidified with 1% formic acid, and standard interface parameters were used to ensure maximal accuracy.

For analysis under nondenaturing conditions, samples were directly infused into the apparatus in 50 mM ammonium acetate (pH 7.0). Interface parameters were optimized to ensure the highest sensitivity and spectrum quality with no effect on the stability of noncovalent complexes. The accelerating voltage applied to the sample cone (V_c) ranged from 30 to 80 V, and the interface pressure was set at 5 mbar. Pressure and V_c control the energy supplied to ions in the interface of the mass spectrometer and must be optimized in each case.

Nonvolatile salts were removed before mass spectrometry, by replacing the sample purification buffer with 50 mM ammonium acetate buffer (>99% pure, Fluka Biochemica) at pH 7.0. Ammonium acetate preserves the native structure of proteins and is compatible with ESI-MS analysis (*44*). Proteins were dialyzed by being spun through a 10 kDa PES Vivaspin microconcentrator (Vivascience, Hannover, Germany) or an Amicon Ultra device (Millipore) at 4 °C. Each spin reduced the volume of the protein sample, and ammonium acetate buffer was then added to bring the sample volume up to its initial level. Under these conditions, each run corresponded to 5-fold dilution of the initial buffer in ammonium acetate buffer. The series of five runs was repeated using a new microconcentrator membrane. During this concentration process, the protein concentration was kept below 80 μM to prevent protein dimerization. The deionized water (18.2 MΩ) used was generated by passage through a special filter (Millipore, Bedford, MA).

The E/EC12, E/D103A, M-E/EC12, and M-E/D103A samples were incubated with several concentrations of Ca^{2+} (added in solution from a 10 mM calcium acetate solution), and the stoichiometry was deduced by mass spectrometry under nondenaturing conditions. These experiments were performed at two different protein concentrations (5 and 15 μM) and at Ca^{2+} concentrations of 0−300 μM.

The free Ca^{2+} concentration in solution was determined by subtracting the quantity of bound Ca^{2+} ions from the total quantity of Ca^{2+} ions in solution. The quantity of bound Ca^{2+} ions was obtained by considering Ca^{2+} binding stoichiometries and assuming that Ca^{2+}-free and Ca^{2+}-saturated cadherin fragments had the same mass spectrometry response factor (*45*). The classical Hill equation was fitted to the experimental data with ORIGIN 7, using a Levenger−Marquart nonlinear least-squares fit procedure.

Binding specificity was assessed by incubating 15 μM M-E/EC12 fragment with several divalent metal ions (135 μM, 9 equiv), and binding stoichiometries were deduced by mass spectrometry under nondenaturing conditions. We used the following divalent metal ions: Ca^{2+} (calcium acetate, >99%, Sigma), Cd^{2+} (cadmium acetate 2-hydrate, >99%, Riedel-de Haën), Mn^{2+} [manganese(II) acetate tetrahydrate, >99%, Fluka Chemica], and Mg^{2+} (magnesium acetate tetrahydrate, >99%, Fluka Chemica).

Trypsin Sensitivity. We incubated purified cadherin fragments (~5 μg) with $CaCl_2$ solutions ranging in concentration from 0.02 to 20 mM in 10 mM Tris (pH 8.0) or with 5 mM EDTA. The protein solutions were then incubated with 90 units of trypsin−agarose beads (Sigma) in a final volume of 40 μL for 1 h, at 37 °C, with shaking (400 rpm, Thermomixer Comfort, Eppendorf). A trypsin inhibitor was added to stop proteolysis (leupeptin hemisulfate, ICN Biomedicals Inc.). Samples were then analyzed by SDS−PAGE in 15% polyacrylamide gels and Coomassie blue staining.

CD Measurements. Circular dichroism (CD) spectra were recorded at 20 °C in a solution containing 20 mM Hepes and 150 mM NaCl (pH 7), using a Jasco 810 spectropolarimeter with quartz cells with a path length of 1 mm. The protein concentration was 0.2 mg/mL. Spectroscopic studies of structural modifications were performed by adding aliquots of a Ca^{2+} stock solution to the Ca^{2+}-depleted protein, to a final Ca^{2+} concentration of 1 mM. The reversibility of the Ca^{2+}-induced modifications was studied by measuring the CD signal after adding EDTA to the same protein solution, up to a final concentration of 2 mM. Spectra were recorded by subtracting the background due to the buffer signal.

RESULTS

Expression and Characterization of Recombinant E-Cadherin Fragments. We studied the Ca^{2+} binding properties of the outermost E-cadherin pocket, using a pair domain fragment, EC12, consisting of the two outermost EC modules comprising this pocket (Figure 1A). Structural studies have identified the amino acids involved in calcium binding, and we know from these studies that Asp103 is involved in coordination of the two outermost calcium ions (Figure 1B and ref *46*). One specific point mutation, Asp103Ala, was introduced to assess the role of Ca^{2+} binding. The E/D103A fragment was designed to have modified Ca^{2+} binding properties (see below). On the basis of the relationship among Ca^{2+} binding, the presence of additional amino acids at the N-terminal end, and EC1 domain stability, we investigated the effect on Ca^{2+} binding of an additional Met residue at the N-terminal end. We designed four chimeric proteins, E/EC12, E/D103A, M-E/EC12, and M-E/D103A, for this part of the study (Figure 1C).

We needed sufficient quantities of highly pure cadherin fragments to obtain relevant quantitative results for Ca^{2+} binding. All four recombinant proteins were overproduced in *Escherichia coli*, as they did not contain glycosylation

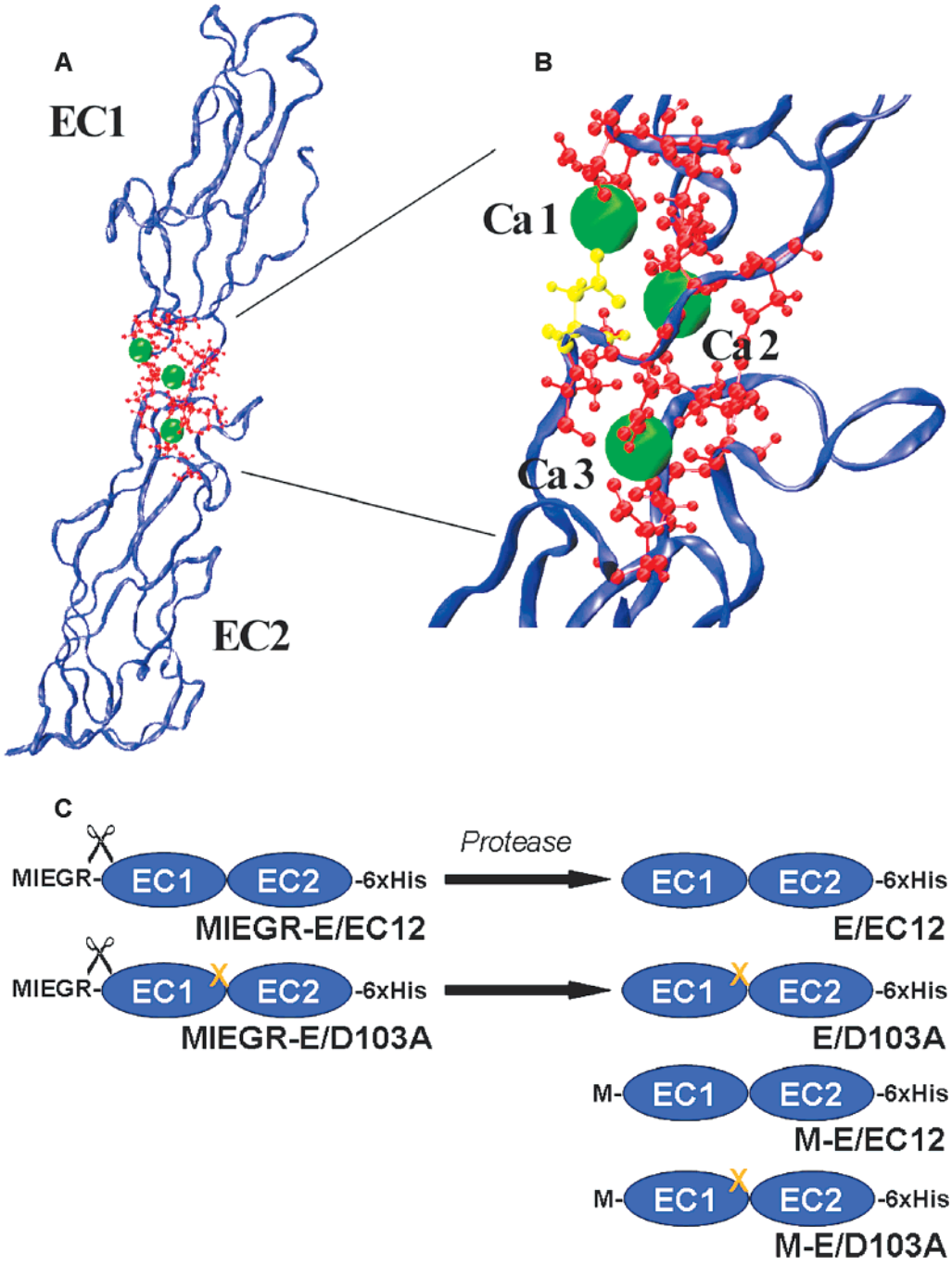

FIGURE 1: (A) Structure of the E-cadherin outermost calcium binding pocket, enclosed between EC1 and EC2 [PDB entry 1EDH (*46*)]. The EC modules are represented as blue ribbons, calcium ions as green spheres, and calcium binding residues as red balls and sticks. (B) Enlargement of the binding site making it easier to visualize the amino acids involved in calcium binding. The Asp103 converted to an Ala in E/D103A is colored yellow. (C) Chimeric cadherin fragments before and after N-terminal end cleavage by factor Xa protease and cadherin fragments with additional N-terminal Met residues. At the C-terminal end of EC2 (last residue, F221), a hexahistidine tag was added to all four recombinant proteins. The orange times sign indicates the D103A point mutation.

motifs. They were then affinity purified on nickel-NTA-Sepharose beads, using their hexahistidine tag. We used SDS−PAGE, Western immunoblotting, and ESI-MS to characterize these protein fragments and to assess their purity.

Only one protein band was detected by Coomassie staining, for all four purified cadherin fragments (Figure 2A and Figure 1 of the Supporting Information). The apparent molecular mass via SDS−PAGE was ~33 kDa, higher than the value predicted from the primary structure (~25 kDa; see below). Only one protein band was detected by Western immunoblotting with the ECCD2 (Takara) and H-15 (Santa Cruz) antibodies specific for an epitope on the EC1 domain and the C-terminal histidine tag on EC2, respectively (data not shown). A small proportion of dimers was observed, due to the presence of a single Cys residue in the sequence.

We also checked the homogeneity of our fragments by ESI-MS. All mass spectra obtained under denaturing (Figure 2B,C) and nondenaturing (Figure 2D,E and Figure 2 of the Supporting Information) conditions showed samples to be highly pure and homogeneous, with the following molecular masses: 25 177.1 ± 0.2 Da for E/EC12, 25 133.0 ± 0.3 Da for E/D103A, 25 308.7 ± 1.0 Da for M-E/EC12, and 25 263.3 ± 1.0 Da for M-E/D103A. These experimental values were consistent with the predicted values: 25 177.0,

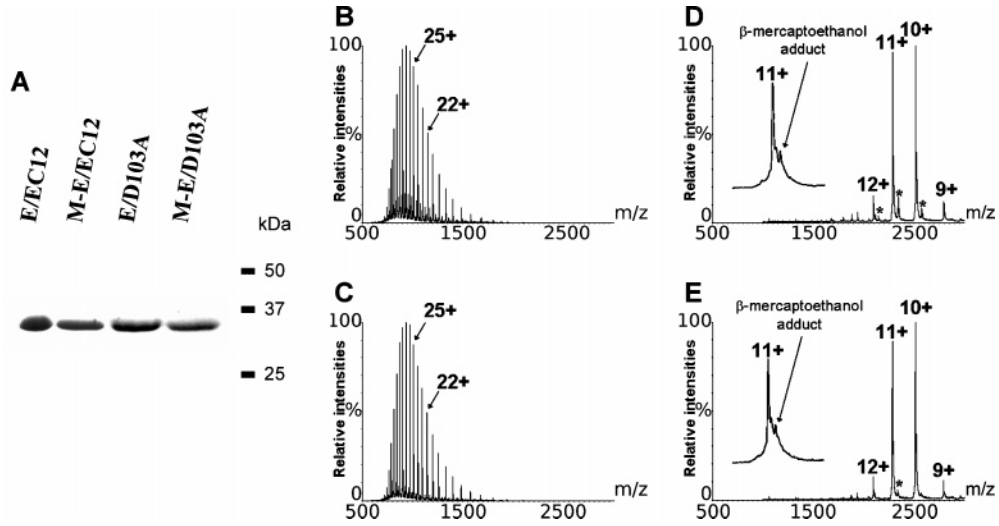

FIGURE 2: Characterization of the cadherin fragments. (A) The purity of M-E/EC12, M-E/D103A, E/EC12, and E/D103A was analyzed by SDS−PAGE followed by Coomassie blue staining. Only one molecular species was detected. (B−E) ESI-MS analysis of E/EC12 and E/D103A. Spectra under denaturing (B and C) and nondenaturing (D and E) conditions, showing different charge state distributions for each protein, as a function of protein folding. Typical charge values are indicated above each distribution. Spectral analysis revealed the presence of a single, homogeneous compound with a molecular mass of 25 177.0 ± 0.2 Da, corresponding to the E/EC12 fragment (M_{rtheo} = 25 177.0 Da), and a single 25 133.0 ± 0.3 Da compound, corresponding to the E/D103A fragment (M_{rtheo} = 25 133.0 Da). A small peak corresponding to one β-mercaptoethanol adduct was also visible (ΔM_r = 76 Da), and residual uncleaved proteins were detected (asterisks).

25 133.0, 25 308.2, and 25 264.2 Da, respectively. A very small proportion of our protein samples had a 76 Da adduct, corresponding to a disulfide bridge formed with the β-mercaptoethanol group present in lysis buffer. This modification, involving Cys9, does not interfere with Ca^{2+} binding (*46*, *47*). We also detected other minor ion series (labeled with an asterisk in panels D and E of Figure 2) corresponding to residual uncleaved proteins (MIEGR-E/EC12 and MIEGR-E/D103A).

The charge state distributions observed on the typically multiply charged ESI mass spectra obtained under denaturing (Figure 2B,C) and nondenaturing conditions (Figure 2D,E) were completely different and related to the conformation adopted by the protein (*48*). Unfolded proteins have been reported to have larger numbers of solvent-exposed amino acids available for protonation than folded proteins, yielding more highly charged ESI ions (lower *m*/*z*). Such variation in charge state distribution could be used to study conformational changes (*49*, *50*) in response to experimental modifications (see below). Two-domain E-cadherin fragments have been shown to be functional in bead−bead and bead−cell aggregation assays and in unimolecular studies using flow chambers and biomembrane force probe approaches (refs *43* and *51* and unpublished data). These cadherin fragments were therefore appropriate for quantitative Ca^{2+} binding studies.

Characteristics of Ca^{2+} Binding. Ca^{2+} ions were added to cadherin fragments in a stepwise manner. Ca^{2+} binding stoichiometries were determined by mass spectrometry under nondenaturing conditions (see Experimental Procedures). Several accelerating voltages (V_c) were used (from 30 to 80 V, data not shown) to ensure that different populations of complexes could be studied in solution. The corresponding stoichiometries were insensitive to accelerating voltage, ruling out the dissociation of Ca^{2+} ions in the gas phase of mass spectrometer and showing that the relative abundance of the species deduced from ESI mass spectra effectively reflected their relative abundance in solution.

Typical mass spectra obtained for E/EC12, E/D103A, M-E/EC12, and M-E/D103A, under different Ca^{2+} conditions, are shown in Figure 3. The binding of 1 molar equiv of Ca^{2+} increases the mass of the protein by 38 Da (as two protons are removed following binding), so all distinct ligation states and unbound cadherin fragments were directly visualized by ESI-MS. The molecular masses obtained showed that all proteins were Ca^{2+}-free in the desalting buffer (Figure 3A,B,G,H). However, E/EC12 and E/D103A displayed different Ca^{2+} binding behavior even at very low Ca^{2+} concentrations. Mass spectra for E/EC12 showed binding to Ca^{2+} at low Ca^{2+} concentrations. Indeed, for a total Ca^{2+} concentration of 45 μM (3 equiv), the mass spectrum indicated two main molecular species, with masses of 25 178.0 ± 1 Da, corresponding to the E/EC12 apoprotein, and 25 292 ± 1 Da, corresponding to the E/EC12$(Ca^{2+})_3$ complex (Figure 3C). During titration, the E/EC12$(Ca^{2+})_1$ and E/EC12$(Ca^{2+})_2$ species were underrepresented with respect to apoprotein and E/EC12$(Ca^{2+})_3$, consistent with cooperative binding. E/D103A seemed to have lost the capacity for cooperative binding, as proportional increases in stoichiometry were observed with the continuous addition of Ca^{2+} ions (Figure 3I). Comparisons of M-E/EC12 and M-E/D103A with E/EC12 and E/D103A, respectively, showed that the presence of an additional N-terminal methionine residue had no effect on Ca^{2+} binding properties (Figures 3 and 4). Finally, stoichiometries of >3 were observed for all fragments, revealing the presence of other Ca^{2+}-binding sites of lower affinity potentially corresponding to the half-binding pocket on the C-terminal side of the EC2 domain (*42*).

Cooperative binding was confirmed by plotting the number of Ca^{2+} ions bound per mole of protein against free Ca^{2+} concentration (see Figure 4). It was then possible to calculate Hill constants from a nonlinear fit of the data and apparent dissociation constants (Ca^{2+}-free concentration at half-saturation). The shape of the Ca^{2+} binding curve indicated a high level of cooperativity for both wild-type proteins (Figure

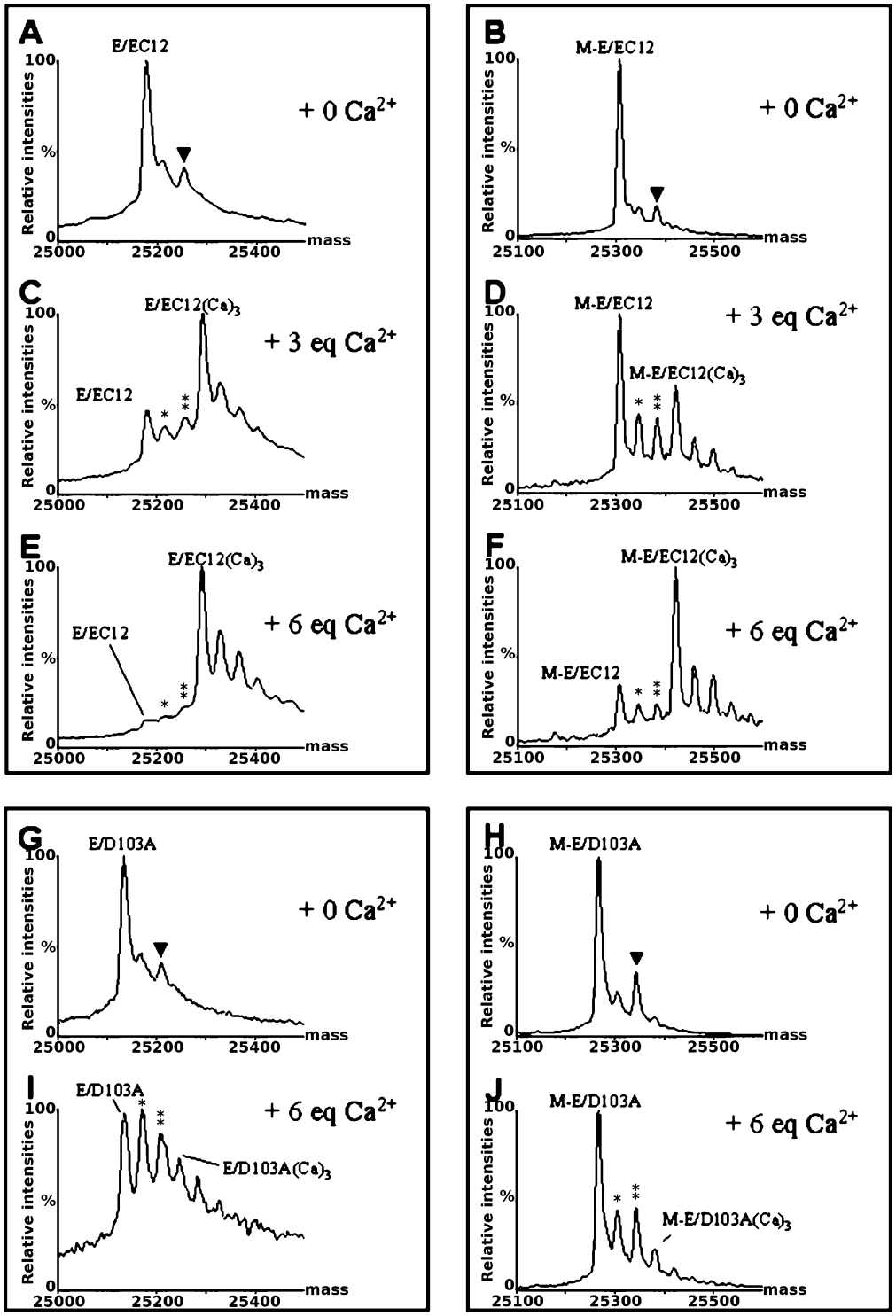

FIGURE 3: Ca^{2+} binding stoichiometries for E/EC12, E/D103A, M-E/EC12, and M-E/D103A determined via ESI-MS under nondenaturing conditions. The experiments presented in this panel were performed by incubating 15 μM protein with 0, 45, and 90 μM Ca^{2+} for E/EC12 and M-E/EC12 (A−F) and 0 and 90 μM Ca^{2+} for E/D103A and M-E/D103A (G−J), respectively. Three Ca^{2+} ions, rather than one (one asterisk) or two (two asterisks), bound preferentially to both E/EC12 and M-E/EC12. This preferential Ca^{2+} binding stoichiometry suggests cooperative binding. By contrast, Ca^{2+} binding seemed to be statistical for both E/D103A and M-E/D103A, suggesting a loss of cooperative binding following the D103A point mutation. A small peak (black arrowhead) corresponding to one β-mercaptoethanol adduct was also visible.

4), which was confirmed by the best fit curve, giving a Hill constant of 2.6 ± 0.2, corresponding to a high level of cooperativity for three calcium ions. An apparent dissociation constant of ~20 ± 0.7 μM for Ca^{2+} binding was obtained for this fit. This result strongly suggests that physiological conditions are sufficient to saturate this cadherin binding pocket. However, binding of Ca^{2+} to the D103A mutated proteins gave a hyperbolic binding curve with a Hill constant of 1.01 ± 0.05, providing evidence of noncooperative binding with an apparent dissociation constant of 240 ± 7 μM.

We evaluated the extent to which other divalent ions (Cd^{2+}, Mn^{2+}, and Mg^{2+}) bound to the wild-type protein by analyzing the formation of the corresponding complexes under nondenaturing conditions. Excess ions were added (135

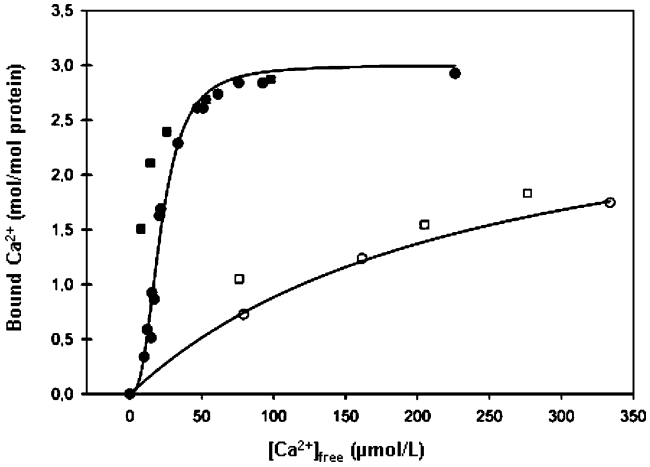

FIGURE 4: Calcium binding to E/EC12 (■), M-E/EC12 (●), E/D103A (□), and M-E/D103A (○), as monitored by ESI-MS under nondenaturing conditions. The number of moles of bound Ca^{2+} per mole of protein is plotted against free Ca^{2+} concentration. The lines correspond to the best fit to these data based on a model of ligand binding to a single class of binding sites.

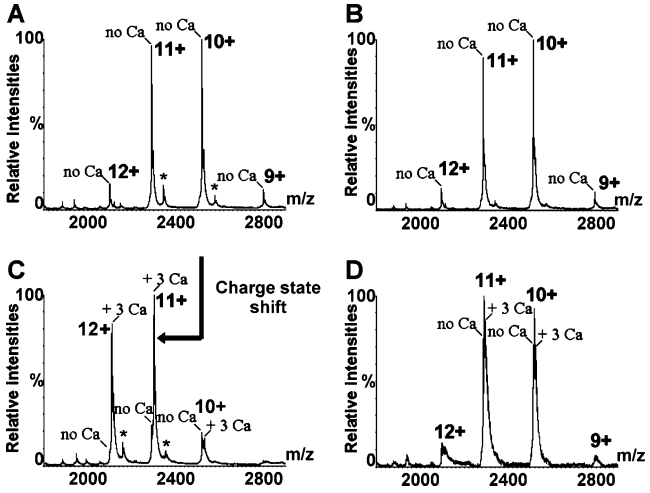

FIGURE 5: ESI-MS spectra of the calcium dependence of E/EC12 and E/D103A charge state distribution under nondenaturing conditions. Experiments were carried out at a protein concentration of 15 μM: (A) Ca^{2+}-free E/EC12, (B) Ca^{2+}-free E/D103A, (C) E/EC12 with 90 μM Ca^{2+} (6 equiv), and (D) E/D103A with 360 μM Ca^{2+} (24 equiv). Ca^{2+}-depleted E/EC12 and E/D103A fragments had similar charge state distributions (main peaks charged +10 and +11), indicating that the D103A point mutation did not disturb the protein charge state distribution. The charge state distribution of E/EC12$(Ca^{2+})_3$ species (C) shifted by one charge (main peaks charged +11 and +12), whereas no change was observed for the E/D103A$(Ca^{2+})_3$ complex (D). Residual uncleaved proteins were also visible (asterisks).

μM, corresponding to 9 equiv). The Ca^{2+}-binding pocket was almost saturated in the presence of excess Ca^{2+}, whereas very little binding was observed following incubation with Cd^{2+}, Mn^{2+}, or Mg^{2+} (data not shown). No Cd^{2+} binding and only small amounts of metal-bound protein for Mn^{2+} and Mg^{2+} (10 and 30%, respectively) were observed. The divalent metal ions tested have patterns of reactivity very similar to that of Ca^{2+} but did not efficiently bind the EC12 fragment. Some divalent ions other than Ca^{2+} do bind, but only at higher (millimolar) concentrations (*20*). Our data suggest that complexes are unlikely to have formed due to experimental artifacts during the ionization process but provide evidence to suggest that EC12 binds Ca^{2+} ions highly specifically.

Structural Rearrangements Require Cooperative Calcium Binding. Two specific pieces of information may be deduced from an ESI mass spectrum: the molecular masses of the various species coexisting in solution and the charge state distribution of the corresponding ions. As molecular mass yields direct information about binding stoichiometries, the charge state distribution is often correlated with protein conformation (*53*−*55*). The number of charges on the observed protein ions depends on the number of basic sites available for protonation and, therefore, on protein folding. E/EC12 and E/D103A had similar charge state distributions under Ca^{2+}-free conditions (Figure 5A,B). The charge state distribution of the wild-type fragment changed following the binding of the three Ca^{2+} ions, whereas that of the E/D103A fragment was barely changed (Figure 5C,D) by Ca^{2+} binding. Similar results were obtained with M-E/EC12 and M-E/D103A (Figure 3 of the Supporting Information). Thus, under identical experimental conditions (in particular pH and interface voltages), the main charge states of E/EC12 shifted from +10−11 to +11−12 following Ca^{2+} binding, whereas the main peak for E/D103A remained unchanged. These data suggest that the observed shift in E/EC12 charge state distribution was related to a change in conformation following cooperative Ca^{2+} binding rather than the number of Ca^{2+} ions bound to the protein. However, no more detail regarding this structural change can be deduced from MS data alone.

We investigated the effects of different Ca^{2+} binding properties on cadherin structure, by analyzing structural modifications of E/EC12, E/D103A, M-E/EC12, and M-E/D103A in protease sensitivity assays and by circular dichroism spectroscopy. One of the key features of cadherins is their resistance to proteolytic degradation in the presence of Ca^{2+} (*17*). Cadherin extracellular segments contain many trypsin cleavage sites but are known to resist proteolysis in the presence of Ca^{2+} but not in the presence of EDTA: trypsin cleavage sites must be buried only in the fully folded protein. We investigated whether the recombinant fragments were correctly folded, and the modulation of their folding and trypsin sensitivity by Ca^{2+}, by subjecting wild-type and modified proteins to trypsin digestion under different Ca^{2+} conditions. The protease resistance of these fragments depends not only on calcium concentration but also on trypsin specific activity and protease/cadherin ratios. The differences in band intensity correspond to experimental fluctuations, due partly to the use of trypsin−agarose beads, which may cause some protein trapping. Thus, protein fragments should be compared solely under identical experimental conditions, without calcium concentrations having any real significance per se. E/EC12 was totally protected from trypsin proteolysis at Ca^{2+} concentrations from 2 to 0.05 mM [no detection of proteolytic fragments with lower molecular masses (Figure 6)]. Under the same experimental conditions, E/D103A was sensitive to proteolysis, even in the presence of 20 mM Ca^{2+}, a concentration 100 times higher than the half-saturation concentration. Similar proteolysis profiles as a function of Ca^{2+} concentration were observed for the M-E/EC12 and M-E/D103A fragments, indicating that the presence of an additional Met residue had no effect on the calcium-dependent folding probed by trypsin sensitivity assays (Figure 4 of the Supporting Information). Differences in

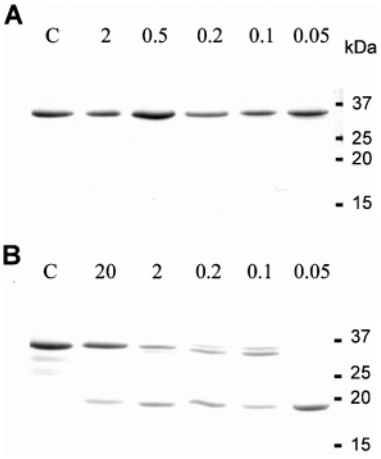

FIGURE 6: Influence of Ca^{2+} on the biochemical properties of E/EC12 (A) and E/D103A (B), as assessed by assays of trypsin sensitivity. Proteins were incubated with trypsin in the presence of various concentrations of Ca^{2+} for 1 h at 37 °C. They were then analyzed by SDS−PAGE in 15% acrylamide gels. Lane C corresponds to the protein incubated without trypsin. Ca^{2+} concentrations (millimolar) are indicated under each subsequent lane. E/EC12 was protected against proteolysis at calcium concentrations exceeding 0.05 mM, whereas E/D103A exhibited no protection, even at a Ca^{2+} concentration of 20 mM. Similar results were obtained with M-E/EC12 and M-E/D103A (see the Supporting Information).

trypsin sensitivity were clearly apparent when protein patterns were compared at the same calcium concentration, with lower-molecular mass degradation peptides observed only with D103A fragments. Thus, calcium binding itself is insufficient to protect cadherin fragments from proteolysis, highlighting the importance of specific cooperative binding.

Circular dichroism spectroscopy was also used to investigate structural changes in wild-type and modified proteins as a function of Ca^{2+} concentration (Figure 7). The mean molar residue ellipticity of E/EC12 was modified by the addition of Ca^{2+} (1 mM) to the protein solution. Similar spectra were observed with only 0.1 mM Ca^{2+}, consistent with our binding data. The spectra obtained following the addition of EDTA (2 mM) showed this structural modification to be reversible. The E/D103A circular dichroism signal was not modified by adding either Ca^{2+} or EDTA. Moreover, E/D103A spectra were similar to spectra of Ca^{2+}-depleted E/EC12 or E/EC12 with EDTA. These observations suggest that Ca^{2+}-depleted E/EC12 and E/D103A have similar secondary structures. Similar results were obtained for M-E/EC12 and M-E/D103A (Figure 5 of the Supporting Information). Thus, the D103A point mutation did not modify the structure of our cadherin apoprotein fragments, as shown by these approaches. Instead, it impaired the native monomer conformation allowed only by cooperative Ca^{2+} binding.

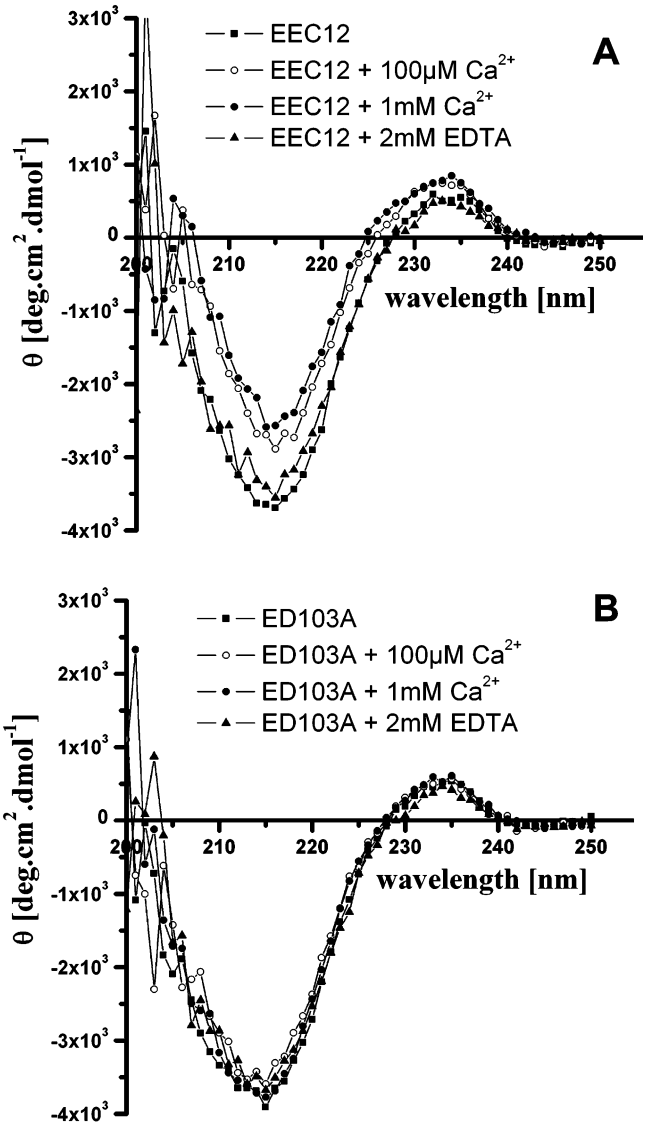

FIGURE 7: Influence of Ca^{2+} on the folding of E/EC12 (A) and E/D103A (B), as studied by circular dichroism spectroscopy. Mean molar residue ellipticity spectra were plotted for each of the following sets of conditions: Ca^{2+}-depleted solution, 100 μM Ca^{2+} solution, 1 mM Ca^{2+} solution, and after the addition of 2 mM EDTA. Ca^{2+} reversibly modified E/EC12 structure but had no effect on the structure of E/D103A. Similar results were obtained with M-E/EC12 and M-E/D103A (see the Supporting Information).

DISCUSSION

Three Calcium Ions Bind Cooperatively to the Outermost Binding Pocket of the Cadherin Monomer. We used four different E-cadherin fragments (E/EC12, E/D103A, M-E/EC12, and M-E/D103A) to investigate Ca^{2+} binding properties as a function of E-cadherin folding. We characterized the specific binding of three calcium ions to the E/EC12 fragment by nondenaturing ESI-MS. Our results were consistent with X-ray crystallographic studies (*46*, *47*) visualizing the binding of these ions at the interface between the EC1 and EC2 domains.

Cadherin−calcium interactions have been studied in various ways, resulting in conflicting findings. Fluorescence spectroscopy and flow dialysis gave an apparent K_D of ~23 μM for binding of Ca^{2+} to MR-E/EC12 (*29*). A constant for binding to M-E/EC12 of 55 ± 3 μM was obtained for the calcium-dependent shift in temperature denaturation profiles (*30*), versus 460 μM estimated from circular dichroism measurements (*28*). Two Ca^{2+}-binding sites with a K_D of 330 μM and a third binding site with a much higher K_D (2 mM) were identified by equilibrium dialysis of M-E/EC12 (*28*). All titration methods are based on indirect or overall measurements, potentially accounting for these discrepancies. Residues on the C-terminal side of EC2 constituting the half-binding pocket bind calcium ions with a lower affinity (*42*), which may affect K_D measurements, depending on the experimental conditions. The main advantage of nondena-

turing ESI-MS is that it allows the direct visualization of different species in solutions at equilibrium. The mean K_D value obtained for the outermost binding pocket in this study (20 ± 0.7 μM) is consistent with fluorescence spectroscopy and flow dialysis measurements (*29*) and strongly suggests that this binding pocket is saturated under physiological conditions, calling into question the notion that cadherin activity is regulated by binding of Ca^{2+} to this pocket.

We detected different stoichiometries coexisting in solution, demonstrating the cooperative binding of three Ca^{2+} ions. This cooperativity was previously suggested by antibody-based (*20*) and structural (*46*, *47*, *56*) studies and was thought to depend on the association of cadherin molecules into dimers (*29*). Our ESI-MS data for the molecular complexes showed that Ca^{2+} ions bound to E/EC12 monomers.

Mutations of the amino acids involved in Ca^{2+} binding profoundly modified the properties of the binding pocket. We used site-directed mutagenesis to replace Asp103 with an alanine. This residue is involved in the binding of two calcium ions (*46*) and has been shown to be important for adhesion of the full-length E-cadherin (*24*). This mutation not only modified binding characteristics (K_D increased from 20 ± 0.7 to 240 ± 7 μM by the D103A mutation), it also abolished cooperativity in calcium binding (Hill coefficient decreased from 2.6 ± 0.2 to 1.01 ± 0.05). Recent studies have suggested that N-terminal β-strand dynamics and Trp2 docking are regulated by Ca^{2+} binding (*14*, *57*). We investigated the effect of additional N-terminal residues on Ca^{2+} binding, using M-E/EC12 and M-E/D103A. The additional Met residue had no significant effect on Ca^{2+} binding. Finally, a comparison between wild-type and D103A mutated proteins strongly suggested that Ca^{2+} binding properties may have exerted a selection pressure leading to cadherin motif conservation.

How Does This Cooperative Binding Influence Structural Properties? Calcium binding contributes to cadherin structure (*15*, *20*, *26*). All four apoproteins, E/EC12, E/D103A, M-E/EC12, and M-E/D103A, had similar structures, with cadherin domains displaying a β-barrel structure. Reversible calcium binding had a marked effect on only E/EC12 and M-E/EC12.

Calcium binding stabilized functional, wild-type, cadherin fragments (ref *43* and Figure 6 of this study), consistent with the known resistance of cadherins to proteolytic degradation in the presence of Ca^{2+} (*17*, *22*). The binding of calcium ions to the D103A fragments (Figure 3) conferred no effective protection against proteolysis. These data show, for the first time, that calcium binding per se is not sufficient to protect cadherin from trypsin degradation. Such protection requires cooperative binding, resulting in a very precise protein conformation.

It has been suggested that Ca^{2+} ions stabilize the otherwise flexible hinge region between two consecutive domains (*46*, *56*). This binding imposes an elongated, rigid rodlike configuration on the molecule, this structure collapsing at Ca^{2+} concentrations of <50 μM (*27*, *42*, *47*). Our ESI-MS measurements provide direct evidence that this structural modification depended on the cooperative properties of Ca^{2+} binding rather than the number of ions bound. The charge state distribution was modified by addition of Ca^{2+} for E/EC12$(Ca)_3$ and M-E/EC12$(Ca)_3$ complexes but not for E/D103A$(Ca)_3$ and M-E/D103A$(Ca)_3$ complexes (Figure 5 and Figure 3 of the Supporting Information). There is a potentially simple explanation for this. In the absence of Ca^{2+}, the hinge region between EC1 and EC2 is highly flexible. Ion binding therefore probably begins on an "open site", on the surface of one module. The complementary surface of the Ca^{2+}-binding site provided by the adjacent module may complete Ca^{2+} binding, due to the flexibility of the hinge region. The binding of a first calcium ion may facilitate the formation of more efficient second and third Ca^{2+}-binding sites, by reducing the relative mobility of the two consecutive cadherin modules. Thus, the cooperative binding of calcium to wild-type cadherin is responsible for the "mature" structure of the functional mature protein and its resistance to proteolysis.

How Does Calcium Binding Regulate Cadherin Function? Several studies have investigated the contribution of calcium to the cadherin-mediated control of cell adhesion.

Depletion of calcium from the extracellular medium leads to the rapid dissociation of cell−cell contacts. Our data strongly suggest that all four E-cadherin calcium-binding pockets are filled even at low calcium concentrations. Indeed, the mean calcium binding parameter obtained for the E/EC12 binding pocket ($K_D = 20 \pm 0.7$ μM) in this study is similar to the global value obtained by Koch et al. for the four binding pockets of the full-length E-cadherin extracellular segment ($K_D = 30$ μM). As the amino acids involved in calcium binding are part of the cadherin motif (*8*, *10*), our findings may be relevant to other members of the cadherin family. Our findings suggest that mechanisms other than cadherin folding may be involved in high-affinity calcium binding under physiological conditions.

Four adhesive interactions with very different stabilities occur in the E-cadherin (*51*) and C-cadherin (*52*) extracellular segments. These interactions involve fine adjustment of the corresponding adhesive interfaces and probably require a very precise geometry of the whole segment. The rigidification observed following Ca^{2+} binding probably increases the level of exposure of adhesive sites at the cell surface, favoring interactions in trans. A similar phenomenon has been reported for other adhesive molecules, such as selectins (*58*, *59*). Calcium-binding sites are functionally important, and single-amino acid substitutions in these sites have been shown to prevent E-cadherin adhesion (*22*, *24*, *60*). Surprisingly, some substitutions create a change in the ectodomain with a stronger effect on adhesion than on protein structure. Indeed, the D103A mutation caused only minor structural modifications (this work), but a considerable loss of adhesion, as shown by cell aggregation assays (*24*). Calcium binding may also be directly involved in the activation of adhesive interfaces. Indeed, calcium may be involved in the β-strand arrangement and stability of cadherin modules, as recently suggested by molecular dynamics analyses (*61*) and observations (*30*). Calcium ions may influence the docking of Trp2 into a hydrophobic pocket, modulating strand exchange between the EC1 domains of opposing cadherins (*15*, *57*).

It remains unclear how Ca^{2+} regulates cadherin activity at the cell surface. Do calcium ions promote the cis dimer formation of E-cadherin molecules on the cell surface, as suggested by Takeda (*62*)? Is calcium required for the formation of trans, but not cis, dimers (*63*)? Our observations do not exclude the possibility that other calcium regulation sites of similar importance are involved in the scaffolding of adhesive plaques (*64*).

The blood calcium concentration is kept stable at 1.4 mM, but local extracellular concentrations in the microenvironment close to the plasma membrane may fluctuate, depending on tissue and stress conditions (see ref *25* for a review). Our results suggest that calcium binding to the cadherin ectodomain should be only mildly affected by such extracellular changes in calcium concentration. Compaction is maintained at 5×10^{-5} M Ca^{2+}, suggesting that this phenomenon is unlikely to be controlled by changes in Ca^{2+} concentration in vivo (*20*). Most studies of cadherin function have been carried out at millimolar calcium concentrations (*15*, *47*, *57*). This does not exclude the possibility that calcium fluctuations may regulate cadherin-mediated cell adhesion. In particular, transient decreases in calcium concentration in the synaptic cleft modify the sensitivity of the cadherin-mediated synaptic plasticity to inhibition (*65*). Moreover, cadherin trans dimers are detectable at 0.1 mM Ca^{2+}; however, their numbers increase at 1 mM Ca^{2+} (*66*), and we have shown here that, at this concentration, more than three Ca^{2+} ions could bind to E/EC12 (Figure 3). These observations are consistent with the calcium sensitivity of cadherin-dependent adhesion being based on mechanisms other than the simple dissociation of cadherin adhesion complexes in the absence of calcium (*11*, *20*, *67*). Adhesion in biology is based on protein−protein recognition, so a detailed knowledge of the way in which calcium modulates cadherin adhesion in vitro may provide important insight into cadherin-mediated adhesion at the cellular level.

ACKNOWLEDGMENT

We thank A. Koch, O. Pertz (J. Engel's laboratory), and I. Lascu (IBGC, Bordeaux, France) for their assistance with circular dichroism experiments, S. Chevalier for his contribution to the table of contents graphic, and J. P. Thiery and D. Loew (Institut Curie) for helpful discussions when this work was initiated.

SUPPORTING INFORMATION AVAILABLE

Data concerning the calcium binding parameters and structure of ME/EC12 and ME/D103A, two cadherin fragments bearing an additional N-terminal methionine residue, SDS−PAGE analysis of the four recombinant proteins used in this study (Figure 1), ESI-MS analysis of M-E/EC12 and M-E/D103A under denaturing and nondenaturing conditions (Figure 2), ESI-MS spectra of their calcium-dependent charge state distribution under nondenaturing conditions (Figure 3), the effect of Ca^{2+} on folding properties, as assessed by trypsin sensitivity (Figure 4), and circular dichroism analyses (Figure 5). This material is available free of charge via the Internet at http://pubs.acs.org.

REFERENCES

1. Larue, L., Antos, C., Butz, S., Huber, O., Delmas, V., Dominis, M., and Kemler, R. (1996) A role for cadherins in tissue formation, *Development 122*, 3185−3194.
2. Pla, P., Moore, R., Morali, O. G., Grille, S., Martinozzi, S., Delmas, V., and Larue, L. (2001) Cadherins in neural crest cell development and transformation, *J. Cell. Physiol. 189*, 121−132.
3. Takeichi, M. (1995) Morphogenetic roles of classic cadherins, *Curr. Opin. Cell Biol. 7*, 619−627.
4. Gumbiner, B. M. (1996) Cell adhesion: The molecular basis of tissue architecture and morphogenesis, *Cell 84*, 345−357.
5. Kemler, R. (1992) Classical cadherins, *Semin. Cell Biol. 3*, 149−155.
6. Nagafuchi, A. (2001) Molecular architecture of adherens junctions, *Curr. Opin. Cell Biol. 13*, 600−603.
7. Steinberg, M. S., and McNutt, P. M. (1999) Cadherins and their connections: Adhesion junctions have broader functions, *Curr. Opin. Cell Biol. 11*, 554−560.
8. Nollet, F., Kools, P., and van Roy, F. (2000) Phylogenetic analysis of the cadherin superfamily allows identification of six major subfamilies besides several solitary members, *J. Mol. Biol. 299*, 551−572.
9. Overduin, M., Harvey, T. S., Bagby, S., Tong, K. I., Yau, P., Takeichi, M., and Ikura, M. (1995) Phylogenetic analysis of the cadherin superfamily allows identification of six major subfamilies besides several solitary members, *Science 67*, 386−389.
10. Patel, S. D., Chen, C. P., Bahna, F., Honig, B., and Shapiro, L. (2003) Cadherin-mediated cell-cell adhesion: Sticking together as a family, *Curr. Opin. Struct. Biol. 13*, 690−698.
11. Shapiro, L., Fannon, A. M., Kwong, P. D., Thompson, A., Lehmann, M. S., Grubel, G., Legrand, J. F., Als-Nielsen, J., Colman, D. R., and Hendrickson, W. A. (1995) Structural basis of cell-cell adhesion by cadherins, *Nature 374*, 327−337.
12. Duguay, D., Foty, R. A., and Steinberg, M. S. (2003) Cadherin-mediated cell adhesion and tissue segregation: Qualitative and quantitative determinants, *Dev. Biol. 253*, 309−323.
13. Gumbiner, B. M. (2005) Regulation of cadherin-mediated adhesion in morphogenesis, *Nat. Rev. Mol. Cell Biol. 6*, 622−634.
14. Haussinger, D., Ahrens, T., Aberle, T., Engel, J., Stetefeld, J., and Grzesiek, S. (2004) Proteolytic E-cadherin activation followed by solution NMR and X-ray crystallography, *EMBO J. 23*, 1699−1708.
15. Koch, A. W., Bozic, D., Pertz, O., and Engel, J. (1999) Homophilic adhesion by cadherins, *Curr. Opin. Struct. Biol. 9*, 275−281.
16. Ozawa, M., and Kemler, R. (1990) Correct proteolytic cleavage is required for the cell adhesive function of uvomorulin, *J. Cell Biol. 111*, 1645−1650.
17. Nose, A., Tsuji, K., and Takeichi, M. (1990) Localization of specificity determining sites in cadherin cell adhesion molecules, *Cell 61*, 147−155.
18. Ringwald, M., Schuh, R., Vestweber, D., Eistetter, H., Lottspeich, F., Engel, J., Dolz, R., Jahnig, F., Epplen, J., Mayer, S., Müller, C., and Kemler, R. (1987) The structure of cell adhesion molecule uvomorulin. Insights into the molecular mechanism of Ca^{2+}-dependent cell adhesion, *EMBO J. 6*, 3647−3653.
19. Troyanovsky, S. (2005) Cadherin dimers in cell-cell adhesion, *Eur. J. Cell Biol. 84*, 225−233.
20. Hyafil, F., Babinet, C., and Jacob, F. (1981) Cell-cell interactions in early embryogenesis: A molecular approach to the role of calcium, *Cell 26*, 447−454.
21. Nose, A., Nagafuchi, A., and Takeichi, M. (1988) Expressed recombinant cadherins mediate cell sorting in model systems, *Cell 54*, 993−1001.
22. Ozawa, M., Engel, J., and Kemler, R. (1990) Correct proteolytic cleavage is required for the cell adhesive function of uvomorulin, *Cell 63*, 1033−1038.
23. Handschuh, G., Candidus, S., Luber, B., Reich, U., Schott, C., Oswald, S., Becke, H., Hutzler, P., Birchmeier, W., Hofler, H., and Becker, K. F. (1999) Tumour-associated E-cadherin mutations alter cellular morphology, decrease cellular adhesion and increase cellular motility, *Oncogene 18*, 4301−4312.
24. Handschuh, G., Luber, B., Hutzler, P., Hofler, H., and Becker, K. F. (2001) Single amino acid substitutions in conserved extracellular domains of E-cadherin differ in their functional consequences, *J. Mol. Biol. 314*, 445−454.
25. Hofer, A. M. (2005) Another dimension to calcium signaling: A look at extracellular calcium, *J. Cell Sci. 118*, 855−862.
26. Boggon, T. J., Murray, J., Chappuis-Flament, S., Wong, E., Gumbiner, B. M., and Shapiro, L. (2002) C-Cadherin ectodomain structure and implications for cell adhesion mechanisms, *Science 296*, 1308−1313.
27. Pokutta, S., Herrenknecht, K., Kemler, R., and Engel, J. (1994) Conformational changes of the recombinant extracellular domain of E-cadherin upon calcium binding, *Eur. J. Biochem. 223*, 1019−1026.
28. Koch, A. W., Pokutta, S., Lustig, A., and Engel, J. (1997) Calcium binding and homoassociation of E-cadherin domains, *Biochemistry 36*, 7697−7705.
29. Alattia, J. R., Ames, J. B., Porumb, T., Tong, K. I., Heng, Y. M., Ottensmeyer, P., Kay, C. M., and Ikura, M. (1997) Lateral self-

assembly of E-cadherin directed by cooperative calcium binding, *FEBS Lett. 417*, 405−408.
30. Prasad, A., and Pedigo, S. (2005) Calcium-dependent stability studies of domains 1 and 2 of epithelial cadherin, *Biochemistry 44*, 13692−13701.
31. Doherty-Kirby, A. L., and Lajoie, G. A. (2002) Investigation of calcium-binding proteins using electrospray ionization mass spectrometry, *Methods Mol. Biol. 173*, 161−174.
32. Hu, P., Ye, Q. Z., and Loo, J. A. (1994) Calcium stoichiometry determination for calcium binding proteins by electrospray ionization mass spectrometry, *Anal. Chem. 66*, 4190−4194.
33. Kaltashov, I. A., Zhang, M., Eyles, S. J., and Abzalimov, R. R. (2006) Investigation of structure, dynamics and function of metalloproteins with electrospray ionization mass spectrometry, *Anal. Bioanal. Chem. 386*, 472−481.
34. Potier, N., Rogniaux, H., Chevreux, G., and van Dorsselaer, A. (2005) Ligand-metal ion binding to proteins: Investigation by ESI mass spectrometry, *Methods Enzymol. 402*, 361−389.
35. Heck, A. J., and Van Den Heuvel, R. H. (2004) Investigation of intact protein complexes by mass spectrometry, *Mass Spectrom. Rev. 23*, 368−389.
36. Loo, J. A. (1997) Studying noncovalent protein complexes by electrospray ionization mass spectrometry, *Mass Spectrom. Rev. 16*, 1−23.
37. Loo, J. A. (2000) Electrospray ionization mass spectrometry: A technology for studying noncovalent macromolecular complexes, *Int. J. Mass Spectrom. 200*, 175−186.
38. Chevreux, G., Potier, N., Van Dorsselaer, A., Bahloul, A., Houdusse, A., Wells, A., and Sweeney, H. L. (2005) Electrospray ionization mass spectrometry studies of noncovalent myosin VI complexes reveal a new specific calmodulin binding site, *J. Am. Soc. Mass Spectrom. 8*, 1367−1376.
39. Craig, T. A., Benson, L. M., Bergen, H. R., Venyaminov, S. Y., Salisbury, J. L., Ryan, Z. C., Thompson, J. R., Sperry, J., Gross, M. L., and Kumar, R. (2006) Metal-binding properties of human centrin-2 determined by micro-electrospray ionization mass spectrometry and UV spectroscopy, *J. Am. Soc. Mass Spectrom. 17*, 1158−1171.
40. Rogniaux, H., Sanglier, S., Strupat, K., Azza, S., Roitel, O., Ball, V., Tritsch, D., Branlant, G., and Van Dorsselaer, A. (2001) Mass spectrometry as a novel approach to probe cooperativity in multimeric enzymatic systems, *Anal. Biochem. 291*, 48−61.
41. Sanglier, S., Bourguet, W., Germain, P., Chavant, V., Moras, D., Gronemeyer, H., Potier, N., and van Dorsselaer, A. (2004) Monitoring ligand-mediated nuclear receptor-coregulator interactions by noncovalent mass spectrometry, *Eur. J. Biochem. 271*, 4958−4967.
42. Haussinger, D., Ahrens, T., Sass, H. J., Pertz, O., Engel, J., and Grzesiek, S. (2002) Calcium-dependent homoassociation of E-cadherin by NMR spectroscopy: Changes in mobility, conformation and mapping of contact regions, *J. Mol. Biol. 324*, 823−839.
43. Perret, E., Benoliel, A. M., Nassoy, P., Pierres, A., Delmas, V., Thiery, J. P., Bongrand, P., and Feracci, H. (2002) Fast dissociation kinetics between individual E-cadherin fragments revealed by flow chamber analysis, *EMBO J. 21*, 2537−2546.
44. Ganem, B., Li, Y., and Henion, J. D. (1991) Detection of noncovalent receptor-ligand complexes by mass spectrometry, *J. Am. Chem. Soc. 113*, 6294−6296.
45. Peschke, M., Verkerk, U. H., and Kebarle, P. (2004) Features of the ESI mechanism that affect the observation of multiply charged noncovalent protein complexes and the determination of the association constant by the titration method, *J. Am. Soc. Mass Spectrom. 15*, 1424−1434.
46. Nagar, B., Overduin, M., Ikura, M., and Rini, J. M. (1996) Structural basis of calcium-induced E-cadherin rigidification and dimerization, *Nature 380*, 360−364.
47. Pertz, O., Bozic, D., Koch, A. W., Fauser, C., Brancaccio, A., and Engel, J. (1999) A new crystal structure, Ca^{2+} dependence and mutational analysis reveal molecular details of E-cadherin homoassociation, *EMBO J. 18*, 1738−1747.
48. Felitsyn, N., Peschke, M., and Kebarle, P. (2002) Origin and number of charges observed on multiply-protonated native proteins produced by ESI, *Int. J. Mass Spectrom. 219*, 39−62.
49. Chowdhury, S. K., Katta, V., and Chait, B. T. (1990) Probing conformational changes in proteins by mass spectrometry, *J. Am. Chem. Soc. 112*, 9012−9013.
50. Konermann, L., and Douglas, D. J. (1998) Unfolding of proteins monitored by electrospray ionization mass spectrometry: A comparison of positive and negative ion modes, *J. Am. Soc. Mass Spectrom. 9*, 1248−1254.
51. Perret, E., Leung, A., Feracci, H., and Evans, E. (2004) Trans-bonded pairs of E-cadherin exhibit a remarkable hierarchy of mechanical strengths, *Proc. Natl. Acad. Sci. U.S.A. 101*, 16472−16477.
52. Bayas, M. V., Leung, A., Evans, E., and Leckband, D. (2006) Lifetime measurements reveal kinetic differences between homophilic cadherin bonds, *Biophys. J. 90*, 1385−1395.
53. Craig, T. A., Veenstra, T. D., Naylor, S., Tomlinson, A. J., Johnson, K. L., Macura, S., Juranic, N., and Kumar, R. (1997) Zinc binding properties of the DNA binding domain of the 1,25-dihydroxyvitamin D3 receptor, *Biochemistry 36*, 10482−10491.
54. Veenstra, T. D., Johnson, K. L., Tomlinson, A. J., Kumar, R., and Naylor, S. (1998) Correlation of fluorescence and circular dichroism spectroscopy with electrospray ionization mass spectrometry in the determination of tertiary conformational changes in calcium-binding proteins, *Rapid Commun. Mass Spectrom. 12*, 613−619.
55. Venters, R. A., Benson, L. M., Craig, T. A., Paul, K. H., Kordys, D. R., Thompson, R., Naylor, S., Kumar, R., and Cavanagh, J. (2003) The effects of Ca^{2+} binding on the conformation of calbindin D(28K): A nuclear magnetic resonance and microelectrospray mass spectrometry study, *Anal. Biochem. 317*, 59−66.
56. Tamura, K., Shan, W. S., Hendrickson, W. A., Colman, D. R., and Shapiro, L. (1998) Structure-function analysis of cell adhesion by neural (N-) cadherin, *Neuron 20*, 1153−1163.
57. Harrison, O. J., Corps, E. M., Berge, T., and Kilshaw, P. J. (2005) The mechanism of cell adhesion by classical cadherins: The role of domain 1, *J. Cell Sci. 118*, 711−721.
58. Hanley, W. D., Wirtz, D., and Konstantopoulos, K. (2004) Distinct kinetic and mechanical properties govern selectin-leukocyte interactions, *J. Cell Sci. 117*, 2503−2511.
59. Huang, J., Chen, J., Chesla, S. E., Yago, T., Mehta, P., McEver, R. P., Zhu, C., and Long, M. (2004) Quantifying the effects of molecular orientation and length on two-dimensional receptor-ligand binding kinetics, *J. Biol. Chem. 279*, 44915−44923.
60. Prakasam, A., Chien, Y. H., Maruthamuthu, V., and Leckband, D. E. (2006) Calcium site mutations in cadherin: Impact on adhesion and evidence of cooperativity, *Biochemistry 45*, 6930−6939.
61. Sotomayor, M., Corey, D. P., and Schulten, K. (2005) In search of the hair-cell gating spring elastic properties of ankyrin and cadherin repeats, *Structure 13*, 669−682.
62. Takeda, H., Shimoyama, Y., Nagafuchi, A., and Hirohashi, S. (1999) E-cadherin functions as a cis-dimer at the cell-cell adhesive interface *in vivo*, *Nat. Struct. Biol. 6*, 310−312.
63. Chitaev, N. A., and Troyanovsky, S. M. (1998) Adhesive but not lateral E-cadherin complexes require calcium and catenins for their formation, *J. Cell Biol. 142*, 837−846.
64. Chan, M. W., El Sayegh, T. Y., Arora, P. D., Laschinger, C. A., Overall, C. M., Morrison, C., and McCulloch, C. A. (2004) Regulation of intercellular adhesion strength in fibroblasts, *J. Biol. Chem. 279*, 41047−41057.
65. Tang, L., Hung, C. P., and Schuman, E. M. (1998) A role for the cadherin family of cell-adhesion molecules in hippocampal long-term potentiation, *Neuron 6*, 1165−1175.
66. Klingelhofer, J., Laur, O. Y., Troyanovsky, R. B., and Troyanovsky, S. M. (2002) Dynamic interplay between adhesive and lateral E-cadherin dimers, *Mol. Cell. Biol. 22*, 7449−7458.
67. Citi, S., Volberg, T., Bershadsky, A. D., Denisenko, N., and Geiger, B. (1994) Cytoskeletal involvement in the modulation of cell-cell junctions by the protein kinase inhibitor H-7, *J. Cell Sci. 107*, 683−692.

BI701340D